Sensors and Actuators Reports 7 (2024) 100184

Contents lists available at ScienceDirect

Sensors and Actuators Reports

journal homepage: www.sciencedirect.com/journal/sensors-and-actuators-reports

Low-cost paper-based sensors modified with curcumin for the detection of ochratoxin a in beverages

Danilo M. dos Santos [a,1], Fernanda L. Migliorini [a,1], Andrey Coatrini-Soares [a], Juliana C. Soares [b], Luiz H.C. Mattoso [a], Osvaldo N. Oliveira [b], Daniel S. Correa [a,*]

[a] Nanotechnology National Laboratory for Agriculture (LNNA), Embrapa Instrumentação, 13560-970 São Carlos, SP, Brazil
[b] São Carlos Institute of Physics, University of São Paulo, São Carlos 13560-970, SP, Brazil

ARTICLE INFO

Keywords:
Paper-based sensor
Curcumin
Ochratoxin a
Electrochemical detection
Optical detection

ABSTRACT

Detection of mycotoxins in food is essential due to their potential harm to human and animal health. However, developing affordable and rapid methods for their detection, particularly with the necessary selectivity to differentiate between various mycotoxins, remains a challenge. Herein, we present low-cost paper-based sensing platforms modified with curcumin, a natural polyphenolic compound, for the electrochemical and optical detection of ochratoxin A (OTA). By exploiting the fluorescence quenching effect of OTA on curcumin through Förster energy transfer, we successfully conducted optical detection with LODs of 0.09 ng mL^{-1} and a linear range of 0.5 to 15 ng mL^{-1}. Additionally, by using electrochemical impedance spectroscopy and a portable instrument, we detected OTA with a limit of detection (LOD) as low as 0.045 ng mL^{-1}. These sensitivity levels meet the requirements established by food regulatory agencies for monitoring food quality in relation to OTA contamination. Our curcumin-modified paper-based sensors offer a compelling combination of simplicity in manufacturing and cost-effectiveness, underscoring their potential for routine food quality monitoring, especially concerning ochratoxin A.

1. Introduction

Ochratoxin A (OTA) is a mycotoxin that can contaminate food and is produced by fungal species such as *Aspergillus carbonarius, Penicillium verrucosum, Aspergillus ochraceus, and Aspergillus niger* [1]. OTA poses significant risks to both humans and animals, as it can cause mutagenic, carcinogenic, teratogenic, hemorrhagic, hepatotoxic, estrogenic, immunotoxic, dermatoxic, nephrotoxic, and neurotoxic effects [2–5]. Contamination with OTA can occur at various stages, including during cultivation, post-harvest, and transportation or storage of food produce. Commonly affected food items include dried fruits, cereals, nuts, corn, oats, coffee, grape juice, wine, wheat, and beer [6–9].

OTA is stable in most food-processing conditions, making it a persistent concern in the realm of food safety [4]. Consumption of OTA-contaminated food has emerged as a substantial public health issue that requires immediate attention. Currently, analytical methods such as enzyme-linked immunosorbent assay (ELISA) [10] and chromatographic assays [11] are employed to detect OTA and monitor food quality. However, these approaches are time-consuming and expensive and require sample preparation and trained personnel to operate the instruments. To address these limitations, alternative systems have been proposed, including electrochemical and optical sensors, which offer simpler procedures for detecting OTA traces [4]. Surface functionalization [5,12,13] can further enhance the performance of these sensors. Notably, paper-based sensors show great promise as they fulfill the requirements for point-of-attention food monitoring, are low-cost, portable, and versatile [14,15]. Additionally, functionalization can be accomplished using a wide range of raw, biodegradable materials [16–18].

In this study, we present an innovative paper-based sensor functionalized with curcumin for the optical and electrochemical detection of ochratoxin A (OTA), as illustrated in Scheme 1. Curcumin is a highly promising sensing element due to its affordability, widespread availability, non-toxicity, and pronounced fluorescence that is quenched in the presence of OTA [19–25]. Notably, curcumin also possesses redox-active properties, with two distinct redox centers: a β-diketone

* Corresponding author.
E-mail address: daniel.correa@embrapa.br (D.S. Correa).
[1] These authors contributed equally to this work.

https://doi.org/10.1016/j.snr.2023.100184
Received 14 October 2023; Received in revised form 24 November 2023; Accepted 17 December 2023
Available online 30 December 2023

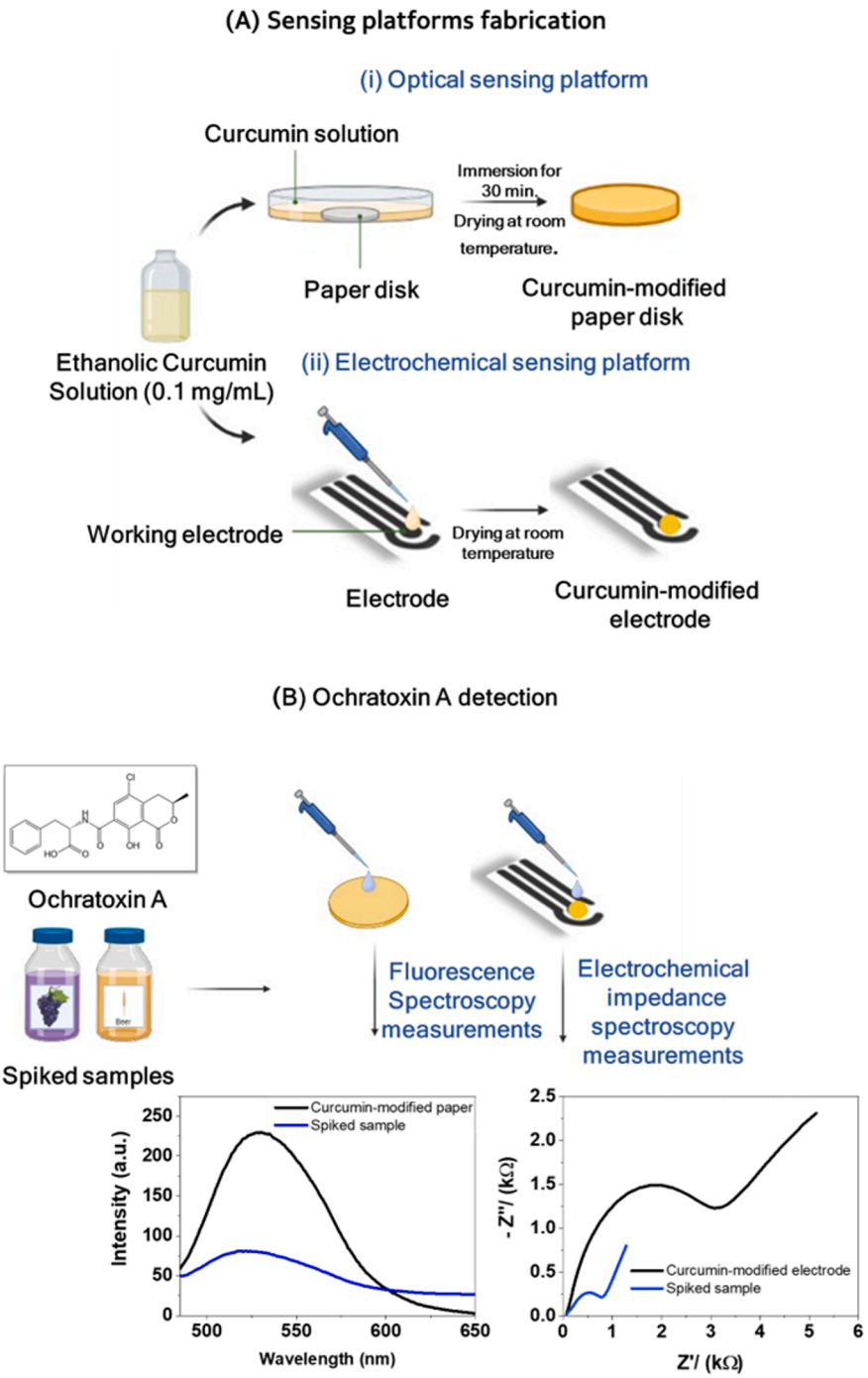

Scheme 1. (A) Schematic representation of the preparation of optical (i) and electrochemical (ii) sensing platforms using a simple approach based on curcumin immobilization on paper substrates. (B) Schematic representation of the application of the curcumin-modified sensing platforms for ochratoxin A detection in grape juice and beer.

moiety and a phenolic hydroxyl group. By leveraging the advantageous optical and electrochemical properties of curcumin, we have successfully fabricated economical and versatile sensors for the precise detection of OTA across a wide range of food matrices. These sensors offer a highly promising solution for efficient and cost-effective OTA detection.

2. Methodology

2.1. Materials

Aflatoxin B1 (AFB1), ochratoxin A (OTA), aflatoxin B2 (AFB2) and Zearalenone (ZEA) were purchased from Sigma-Aldrich. Shellac was acquired from Acrilex® (São Bernardo do Campo/SP, Brazil), while graphite, carbon black and absolute ethanol were obtained from Synth (Diadema/SP; Brazil) and Cabot (Boston/Massachusetts; USA), respectively. Adhesive paper used as substrate was purchased from PIMACO

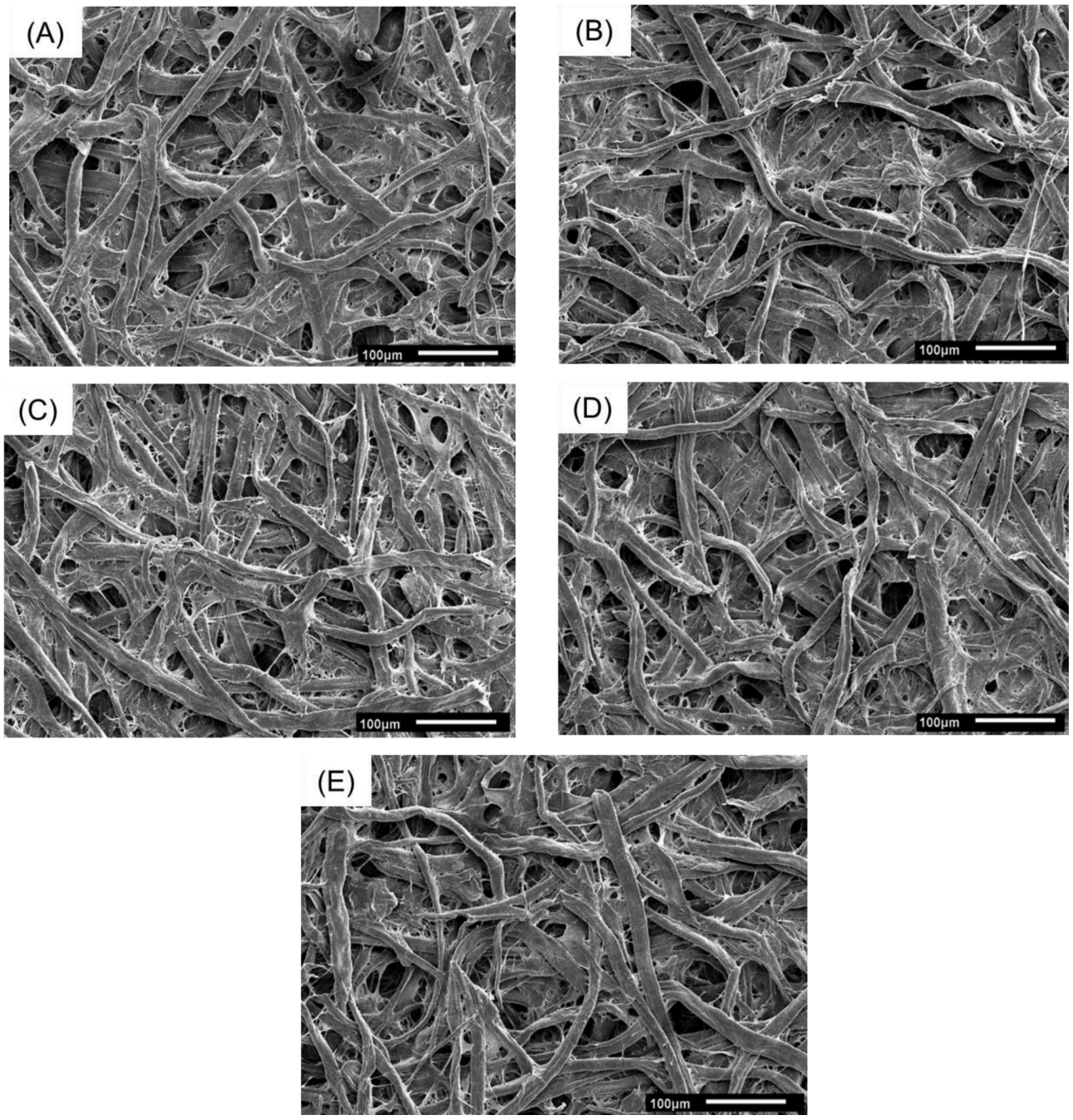

Fig. 1. SEM images for paper disks before (A) and after (B) modification with ethanolic curcumin solution; paper disk modified with curcumin after contact with OTA solutions at concentrations 2.5 ng mL^{-1} (C), 50 ng mL^{-1} (D), 100 ng mL^{-1} (E).

(A4 ink-jet/laser 288.5 × 200.0 367 BIC, Brazil) and crystal acetate sheet used as a substrate for placing adhesive paper was purchased from Artigianato A4, Brazil. Disks of quantitative filter paper (JP40- with 80 g cm^{-2} density and average pore size of 25 µm) used as substrate of optical sensing platform were acquired from J. Prolab (Paraná, Brazil). Curcumin (Cur) was purchased from Sigma-Aldrich (Saint Louis, MO, USA).

2.2. Preparation of optical and electrochemical sensors based on curcumin

To prepare the optical sensor (Scheme 1A (i)), disks of quantitative filter paper (~1 cm diameter) (JP40) were cut and immersed in curcumin dissolved in ethanol (0.1 mg mL^{-1}) for 30 min. The modified paper disks were dried at room temperature and stored in the dark to prevent photobleaching of curcumin.

The electrochemical platform (Scheme 1A (ii)) was prepared using a simple, low-cost cut-printing process with slight modifications to the methodology described in a previous study [26]. A thin layer of conductive ink made of a suspension of graphite/carbon black powder (90/10 (w/w)) in shellac at a proportion of 30 % (w/w) was deposited homogeneously onto the adhesive paper and then dried at 40 °C for 1 h in an air-circulating oven. A cut printer (Silhouette, model 3, Moema/SP, Brazil) was used to cut a mask with working (diameter = 3.3 mm), counter, and reference electrodes from the conductive sheets. The mask was then removed and glued to a flexible and waterproof acetate sheet. The functionalization of the working electrode was performed by dripping a solution of curcumin (0.1 mg mL^{-1}) dissolved in ethanol, which was then dried at room temperature and stored in the dark to

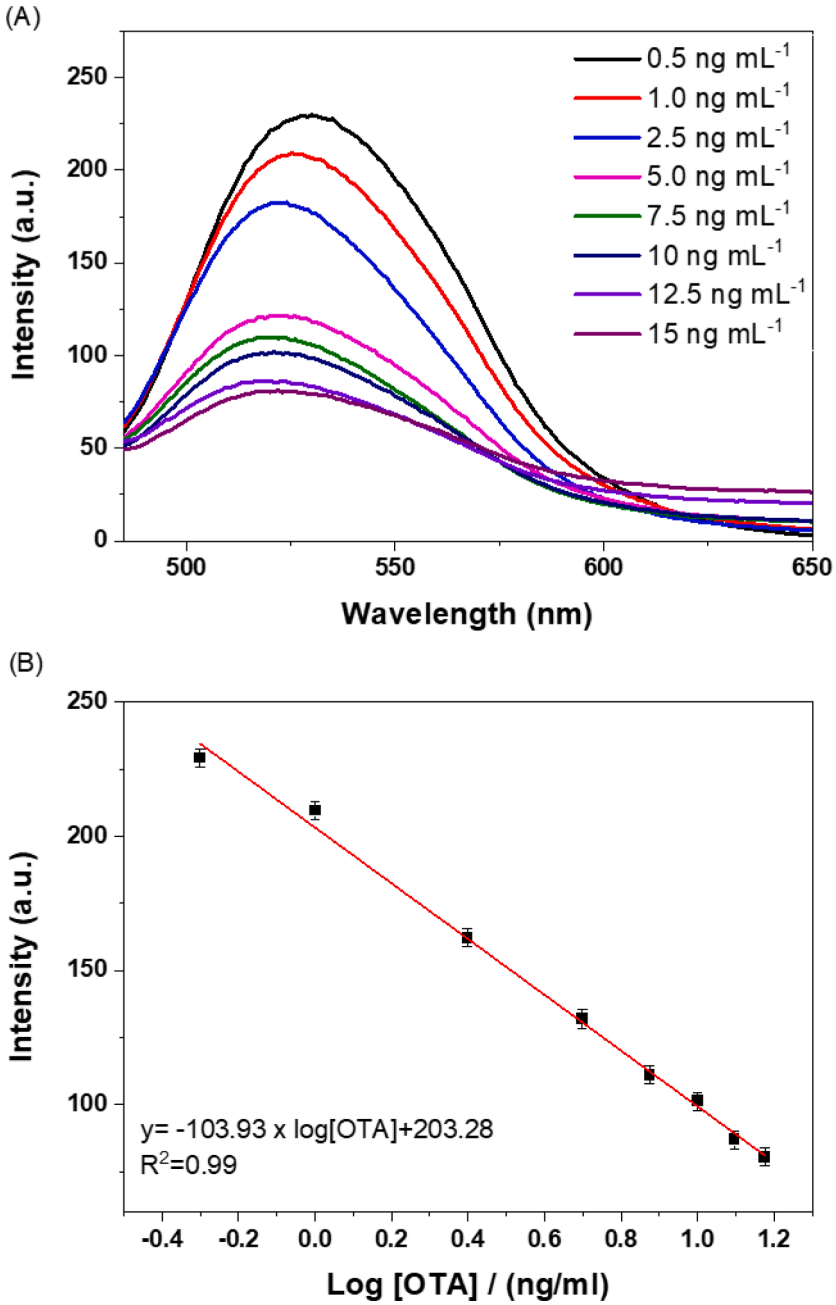

Fig. 2. Fluorescence spectra of curcumin-modified paper disks exposed to different OTA concentrations (A) and fluorescence intensity × logarithm of OTA concentration (B) in the linear range of 0.5 to 15 ng mL^{-1}.

prevent photobleaching.

2.3. Characterization of the sensors after modification with curcumin

The morphology of the paper-based sensors was characterized using scanning electron microscopy (SEM, JEOL 6510) at an acceleration voltage of 10 kV. Before the analyses, samples were coated with a thin layer of gold using a sputter coater (Leica). To study interaction mechanisms, polarization-modulated infrared reflection absorption spectroscopy (PM-IRRAS) measurements were carried out on gold substrates functionalized with curcumin films. The spectra were acquired with a PMI 550 spectrophotometer (KSV Instruments, Helsinki, Finland), with an incident angle of 81° and spectral resolution of 8 cm^{-1}. The PM-IRRAS signal was obtained through Eq. (1), where R_S and R_P are, respectively, reflectivity of the parallel and perpendicular component to the plane of incidence of the IR light.

$$\frac{\Delta R}{R} = \frac{R_S - R_P}{R_S + R_P} \quad (1)$$

2.4. Preparation of solutions for the optical and electrochemical detection of OTA

For optical detection an OTA stock solution in dimethylsulfoxide (DMSO) (1 mg mL^{-1}) was used to prepare aliquots diluted in absolute ethanol which had concentrations in two ranges, from 0.5 to 15 ng mL^{-1} and from 20 to 100 ng mL^{-1}. The electrochemical detection was carried out from an OTA stock solution in 10 mM PBS (pH 7.4) (1 mg mL^{-1}) used to prepare aliquots diluted in one range, from 0.5 to 15 ng mL^{-1}.

2.5. Optical and electrochemical detection of OTA

The optical detection of OTA was performed by dripping 20 μL OTA solutions at different concentrations on one of the sides of paper disks modified with curcumin, which were then dried at room temperature in the dark. Fluorescence measurements were carried out to detect the analyte using a commercial fluorimeter (FluoroLog SPEX/1680, 0.22 m) using a Xenon lamp (Xe) as excitation source and varying the excitation between 450 and 650 nm. The excitation spectra were collected at λ_{em} = 470 nm. For the electrochemical detection experiments, 100 μL of OTA solution of distinct concentrations were dripped onto the working electrode. Electrochemical impedance spectroscopy measurements (EIS) were performed using a hand-held potentiostat (PalmSens4, PalmSens BV, The Netherlands) controlled with PStouch app installed on a smartphone. The EIS experiments were carried out by applying a 10 mV AC voltage in the frequency range from 0.1 Hz to 10 kHz under an open circuit potential (OCP).

2.6. Data analysis with an information visualization technique

The analysis of the large amount of data generated during biosensing experiments can be improved with the use of projection techniques that reduce the data dimensionality, allowing the assessment of selectivity and the possible presence of false positives. Herein, Nyquist plots obtained from commercial OTA samples and OTA samples in grape juice/beer were processed with the Interactive Document Mapping technique (IDMAP) [27]. This technique projects the Nyquist spectra in a lower dimension space $Y = \{y_1, y_2, y_3, \ldots, y_n\}$ from the Euclidean distance between the samples in the original space $X = \{x_1, x_2, x_3, \ldots, x_n\}$ [28]. The error function is given by Eq. (2):

$$Error_{IDMAP} = \frac{\delta(x_i, x_j) - \delta_{min}}{\delta_{max} - \delta_{min}} - d(y_i, y_j) \quad (2)$$

where $\delta(x_i,x_j)$ and $d(y_i,y_j)$ are the Euclidean distances in the original and lower dimensional spaces, respectively, and $\delta_{max}/\delta_{min}$ are the maximum/minimum Euclidean distances between the data instances in the original representation space [28,29].

3. Results and discussion

3.1. Optical detection

The morphological integrity of the paper disks employed in our sensor platform remained unaltered throughout our experimentation, even following curcumin incorporation and exposure to varying OTA concentrations, as evidenced by the SEM images presented in Fig. 1. The initial SEM image in Fig. 1A portrays a characteristic heterogeneous, fibrous, and rough surface of the untreated paper substrate. Remarkably, this morphology remained unchanged after exposure to OTA at different concentrations (Fig. 1C–E), underscoring the sensor's stability in aqueous media.

Figs. 2(A) and (C) depict the fluorescence spectra obtained in triplicate from curcumin-modified paper disks after exposure to varying OTA concentrations in two distinct spectral ranges. A trend was observed where the emission band decreased as the OTA concentration increased, as highlighted in Fig. 2(B) and (D). This phenomenon is attributed to a dynamic quenching process via Förster mechanism, where the excited-state donor (curcumin) transfers energy non-radiatively to the acceptor (OTA) through long-range dipole-dipole interactions between the two molecules [30–32].

Quantitative analysis using linear regression yielded a equation that models the correlation between fluorescence intensity and OTA concentration within the 0.5 to 15 ng mL^{-1} range. The equation, expressed as y = -103.93 × log [OTA] (ng mL^{-1}) + 203.28, demonstrates a high coefficient of determination (R^2 = 0.99). The limit of detection (LOD) was calculated as 0.09 ng mL^{-1} (0.09 ppb) using the 3.3σ/S formula, where σ is the standard deviation of three measurement responses using a fixed concentration of OTA solution, and S is the slope of the calibration curve [33,34]. Significantly, these LOD fall below the maximum OTA levels permitted by regulatory agencies, such as the European Food Safety Authority (EFSA) [5], and Brazilian legislation [35], thereby confirming the sensor's suitability for rigorous food safety standards. We also conducted reproducibility assessments, both inter-sensor and intra-sensor, using curcumin-modified paper disks and OTA solutions at concentrations of 0.5–15 ng mL^{-1}. The relative standard deviation (RSD) for a single electrode was 1.66 % and increased to 4.28 % when three identical electrodes were used.

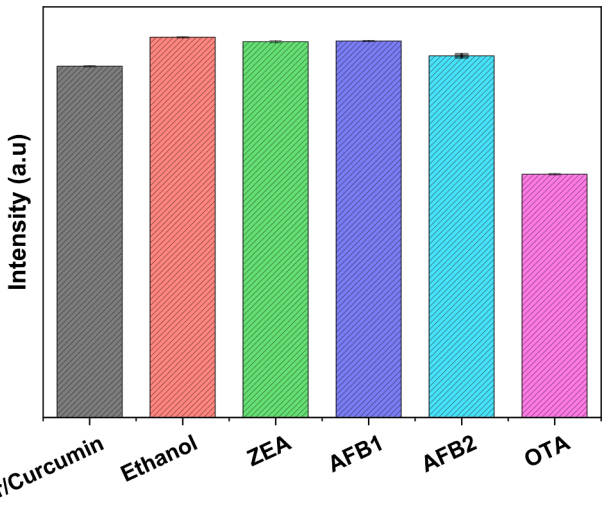

Fig. 3. Fluorescence intensity at the bands for curcumin-modified paper-based sensors for OTA detection in the absence and presence of other interfering mycotoxin (ZEA, AFB1, AFB2 (1 ng mL^{-1})) and ethanol.

To assess the applicability of our curcumin-modified paper disks, we evaluated their performance in detecting OTA in grape juice and beer, two beverages that are susceptible to mycotoxin contamination. We employed the spiked sample method [12,26,36], introducing a known quantity of analyte into the sample before analysis. The recovery rate was determined by comparing the measured analyte amount in the spiked sample to the known amount added, expressed as R = (measured amount of analyte / true amount of analyte) × 100 %. Our results demonstrate that the sensors exhibited high recovery rates of 99 % and 104 % in beer and grape juice spiked with OTA (1 ng mL^{-1}), respectively, demonstrating their robustness in complex beverage matrices. Furthermore, we evaluated the selectivity of our sensors in the presence of other common mycotoxins found in food, including aflatoxin B1 (AFB1), aflatoxin B2 (AFB2), and Zearalenone (ZEA), as well as ethanol, which was used as the solvent for OTA solutions. Our fluorescence spectra analysis (Fig. 3) demonstrates that the fluorescence intensity at the peak (λ= 470 nm) remains nearly consistent for ethanol and the interferents, slightly exceeding that of the curcumin-containing paper sensor. This observation aligns with the dynamic quenching process via Förster mechanism, where the efficiency of analyte-sensor interaction is influenced by the extent of electron transfer processes [32,37]. Given the structural similarity between OTA and curcumin, we propose that the dynamic quenching process via the Förster mechanism is more efficient in the presence of OTA, providing a rational basis for the selectivity of our platform toward this specific mycotoxin. Consequently, the lowest intensity observed for OTA confirms the selectivity and suitability of the sensor for OTA detection in complex food matrices.

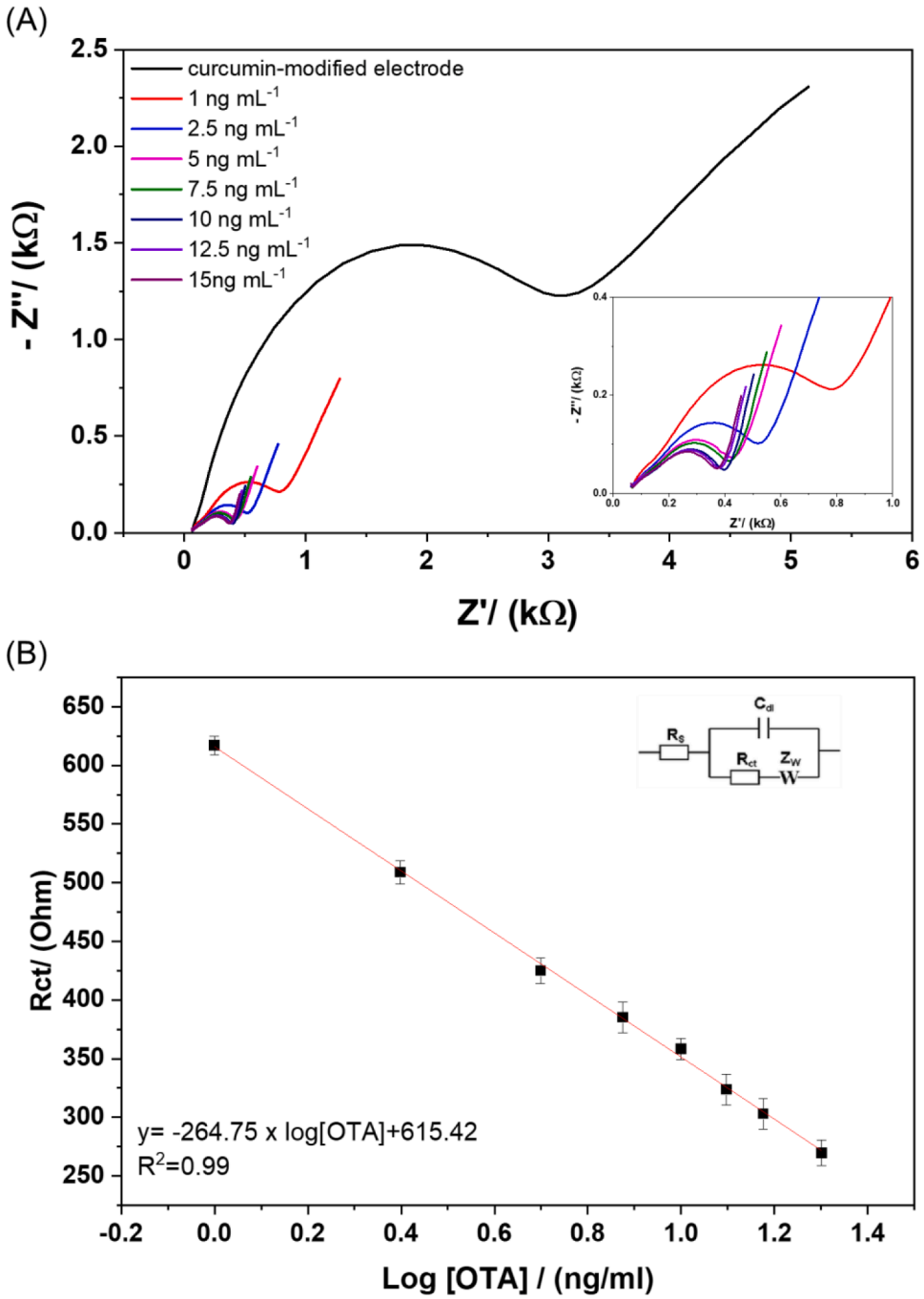

Fig. 4. (A) Nyquist plots derived from electrochemical impedance spectroscopy (EIS) measurements of curcumin-modified paper sensors exposed to varying concentrations of OTA in standard solutions. (B) Rct × logarithm of OTA concentration from 1 to 15 ng mL^{-1}. The inset shows the equivalent circuit model used to fit the impedance data [38].

3.2. Electrochemical detection

Electrochemical impedance spectroscopy (EIS) is a powerful electrochemical technique for investigating interfacial properties and electron transfer kinetics. It involves measuring the impedance of an electrode-solution interface as a function of frequency. The resulting Nyquist plots can be analyzed using equivalent circuits to extract information about the charge transfer resistance (Rct), interface capacitance (Cdl), and Warburg impedance (Zw) [38]. In this study, EIS was used to investigate the electrochemical behavior of OTA at the interface of a curcumin-modified electrode. To enhance the sensitivity of the fabricated electrodes prior to surface modification, we employed electrochemical activation, as described in our previous work [26]. This procedure involved using cyclic voltammetry in 0.05 mol L^{-1} H_2SO_4 within a potential range of −1.5 V to 1.5 V at a scan rate of 50 mV s^{-1} for one cycle. Curcumin was employed to augment the sensitivity and selectivity of EIS-based OTA detection due to its ability to form complexes with OTA molecules, enhancing the binding affinity between OTA and the electrode surface [32]. Consequently, the presence of OTA in the electrolyte solution induces a more pronounced change in the impedance of the double layer, which can be more readily detected by EIS. The Nyquist plots obtained after exposing the electrode to OTA solutions exhibited a high-frequency semicircle characteristic of interfacial charge transfer. The semicircle diameter increased with increasing

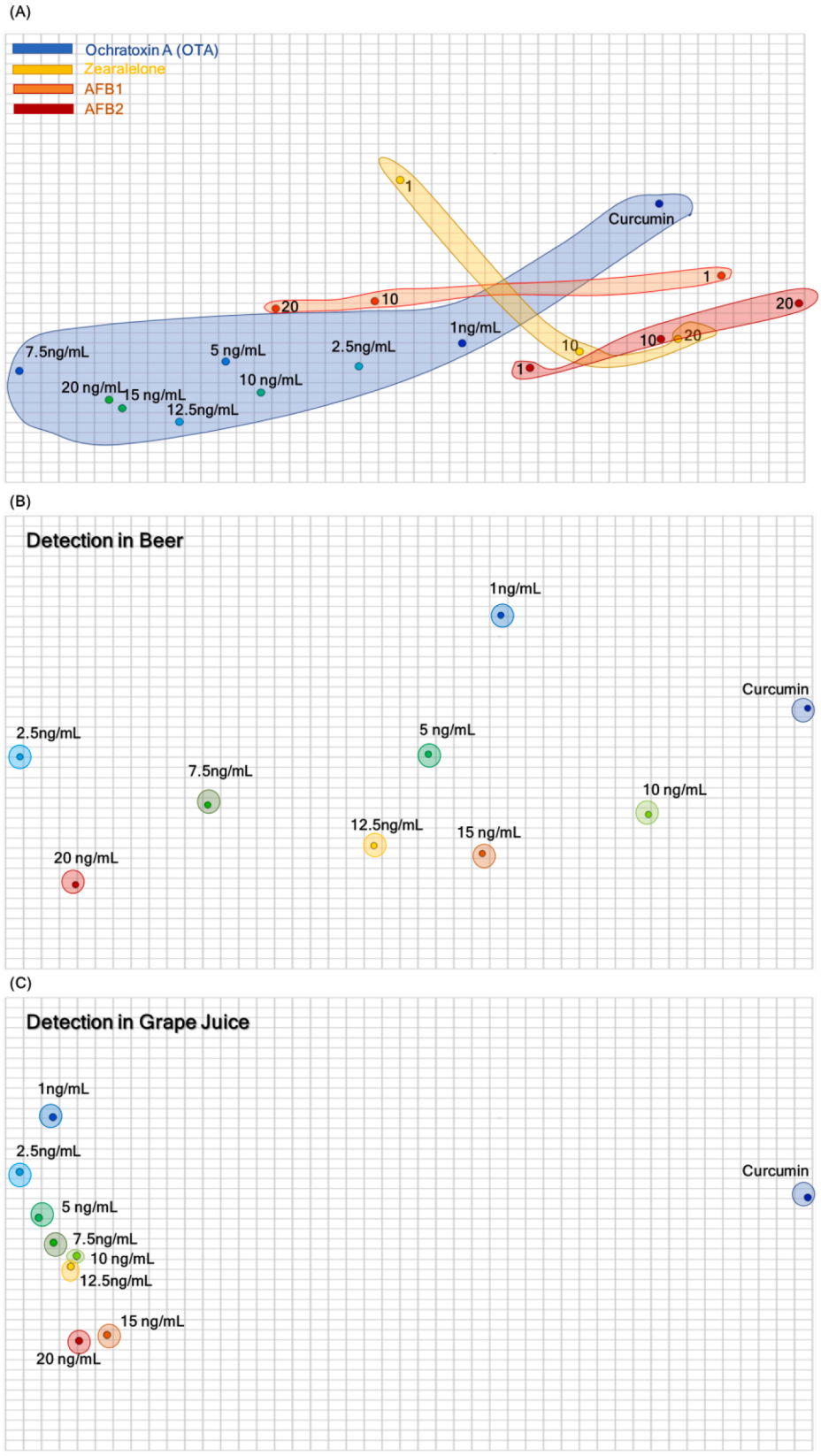

Fig. 5. (A) IDMAP plot using Nyquist data for different OTA concentrations and interferents (AFB2, AFB2, Zearalelone). The sample named curcumin represents the curcumin-containing paper sensor exposed to a blank in an aqueous 10 mM PBS (pH 7.4) solution (0 ng mL^{-1}). The other samples in the blue cluster are OTA dissolved in DMSO at different concentrations. (B) IDMAP plot using Nyquist data for different concentrations of OTA in beer dissolved in aqueous 10 mM PBS (pH 7.4), with a Silhouette Coefficient of 0.771. (C) IDMAP plot using Nyquist data for different concentrations of OTA in grape juice dissolved in aqueous 10 mM PBS (pH 7.4), with a Silhouette Coefficient of 0.786.

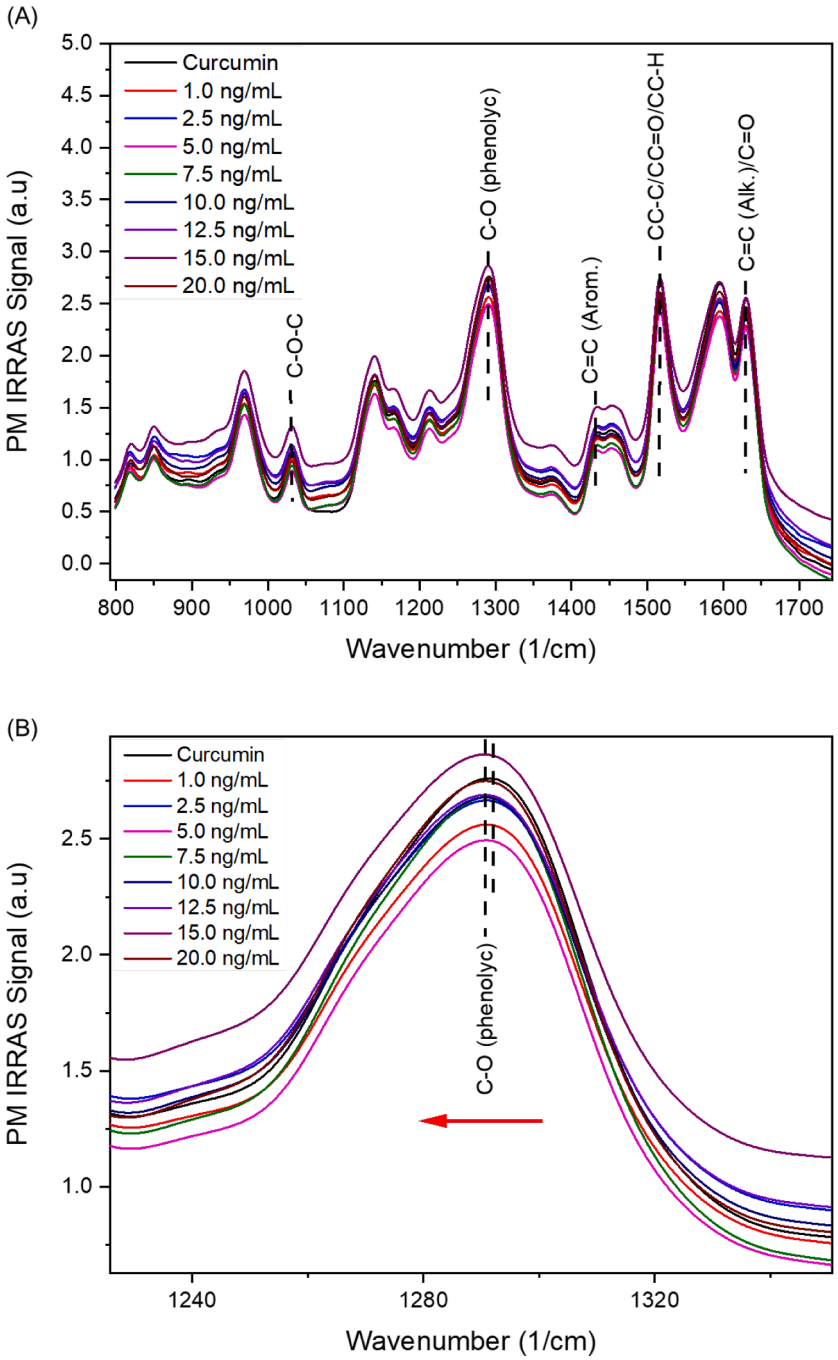

Fig. 6. (A) PM-IRRAS spectra of the curcumin layer exposed to various OTA concentrations in aqueous 10 mM PBS (pH 7.4) solution, including the spectrum for the sensor itself (zero concentration). The gold spectrum was used as the reference spectrum before being coated with a curcumin layer. (B) PM-IRRAS spectra in the range of 1225–1350 cm^{-1}, showing band shifts to smaller wavenumbers upon interaction between OTA and curcumin.

OTA concentration, indicating a decrease in the charge transfer rate. This reduction can be attributed to the adsorption of OTA molecules onto the electrode surface, hindering the active sites for electron transfer.

The linear region at low frequencies in the Nyquist plots is indicative of diffusion-controlled processes. The slope of the linear region decreased with increasing OTA concentration, indicating a decrease in the diffusion coefficient of OTA. A calibration curve was constructed by plotting Rct as a function of OTA concentration. The calibration curve was linear with a high correlation coefficient ($R^2 = 0.99$), indicating that the electrochemical method is sensitive to OTA. The limit of detection (LOD) of the method was calculated to be 0.045 ng mL^{-1}, which is significantly lower than the maximum allowable limits of OTA in food and beverages set by various regulatory agencies. The intra-electrode and inter-electrode reproducibility of the electrochemical method was assessed by performing consecutive measurements using the same electrode and different electrodes, respectively. The relative standard deviation (RSD) was 1.09 % for intra-electrode experiments and 5.33 % for inter-electrode measurements. These low RSD values indicate that the electrochemical method is reproducible. Overall, the EIS results demonstrate that the curcumin-modified electrode is a promising platform for the development of a sensitive and reliable electrochemical sensor for OTA detection.

The excellent analytical performance was confirmed by analyzing

Table 1
Comparison among electrochemical and optical sensors for OTA in the literature.

Detection method	Linear Range (ng ml^{-1})	Detection Limit (ng ml^{-1})	Reference
Optical	0.5–80	0.33	[45]
Optical	1–1000	1.0	[46]
Optical	8–202	6.66	[47]
Electrochemical	0.3–20	0.37	[48]
Electrochemical	0.01–5	0.01	[49]
Electrochemical	0.01–10	0.003	[50]
Optical/	0.5–15/ 20–100	0.09/0.12	This work
Electrochemical	1–15	0.045	This work

Nyquist plots of OTA commercial samples with interferents, and OTA diluted in grape juice and beer, using the multidimensional projection technique IDMAP. This approach allows us to visually represent each Nyquist plot as a distinct marker on a two-dimensional map. The spatial arrangement of these markers accurately reflected the dissimilarities among the various samples analyzed. The discerning power of our methodology is shown in Fig. 5(A). OTA samples stand out prominently from other mycotoxins such as AFB1, AFB2, and ZEA. Notably, the OTA concentrations typically shifted from right to left on the map, showing a clear trend. However, it is important to note that a few false positives may arise in cases involving low OTA concentrations (e.g., 1 ng mL^{-1}) and the presence of AFB1, AFB2, or ZEA.

To validate the effectiveness of the developed electrochemical sensing platform for OTA detection in beverage matrices, we analyzed Nyquist plots obtained from EIS measurements of curcumin-modified paper sensors exposed to varying OTA concentrations in 100-fold diluted (A) beer and (C) grape juice beverages [36]. The Nyquist plots and their corresponding Rct values are presented in Figure S1. Consistent with the observed behavior in PBS solution (pH = 7.4) (Fig. 4), the charge transfer resistance (Rct) values for diluted beverage samples also exhibited a decreasing trend with increasing OTA concentration. This observation suggests the absence of significant interference from quenching components in the analyzed beverages, highlighting the robustness and reliability of the proposed sensing platform. The IDMAP plots corresponding to the measurements in diluted beer and grape juice are shown in Figs. 5(B) and 5(C), respectively. These plots clearly demonstrate the sensor's ability to discriminate between varying OTA concentrations in both beverage types. To quantify this distinction, we employed the silhouette coefficient methodology [39,40]. The calculated silhouette coefficients yielded \values of 0.771 and 0.786 for beer and grape juice, respectively. These values indicate a high degree of separation between distinct OTA concentrations within each beverage, demonstrating that our sensor exhibits good analytical performance for OTA detection in beverage samples.

3.3. Adsorption mechanism behind detection

Polarized-Modulated Infrared Reflection Absorption Spectroscopy (PM-IRRAS) [41,42] was employed to provide valuable insights into the OTA detection mechanism by observing changes in spectral bands associated with both OTA and curcumin. In Fig. 6(A), we present spectra obtained from gold substrates coated with a curcumin layer and exposed to various concentrations of OTA in an aqueous 10 mM PBS solution at pH 7.4. In this figure, the characteristic bands of curcumin and OTA [43,44] are clearly highlighted, aiding in our analysis. Of particular significance is the observation in Fig. 6(B) where the C—O (phenolic) band at approximately 1290 cm^{-1} [43], linked to curcumin, undergoes a noticeable shift towards smaller wavenumbers upon interaction with OTA. It is important to note that this shift is not solely proportional to OTA concentration, as variations in molecular dipole orientation may also impact band area and intensity. This complex interplay suggests that the extent of analyte-sensor interactions, including electron transfer processes, plays a pivotal role in this context. Our hypothesis centers on the molecular structural resemblance between OTA and curcumin, and its ability to interact, enhancing the efficiency of the dynamic quenching process via the Förster mechanism, providing a compelling rationale for the selectivity of our proposed platform towards OTA. Furthermore, when curcumin is employed as a sensing probe for electrochemical OTA detection, the structural parallels between these compounds foster interactions driven by dipole-dipole and van der Waals intermolecular forces. This synergistic interaction pattern substantially boosts the sensitivity of our sensing platform to OTA [32,37].

3.4. Estimate of the sensor cost and comparative study with other sensors

Table 1 presents a comparative analysis of the limits of detection (LODs) for curcumin-containing paper sensors in contrast to previously reported electrochemical and optical sensors. The noteworthy aspect here is the competitive performance of the curcumin-based paper sensors, especially considering their straightforward design and inherent selectivity. A remarkable feature of these sensors is their ability to target ochratoxin A (OTA) without the need for antibody immobilization, simplifying the sensing process. Furthermore, the economic viability of these sensors is a key highlight. The estimated material expenses stand at US$ 0.35 per 100 units for fluorometric sensors and US$ 0.50 per 100 units for electrochemical sensors. Notably, the fabrication process itself is cost-effective, making these sensors not only robust in their analytical capabilities but also an attractive choice from a budgetary standpoint.

4. Conclusions

We have developed versatile, cost-effective, and disposable sensing platforms for ochratoxin A (OTA) detection in food using curcumin as the sensing molecule. Our sensors exhibit good sensitivity, with limits of detection (LODs) of 0.09 ng/mL and 0.045 ng/mL for optical and electrochemical transduction methods, respectively. These sensors retain their efficacy in detecting OTA across a range of food matrices, even in the presence of potential interferents. Their robust performance is validated by multidimensional projection techniques, such as IDMAP, for processing electrochemical data. A key feature of our sensors is their ability to reliably discriminate OTA from other common interfering mycotoxins, such as aflatoxin B1, aflatoxin B2, and zearalenone. This capability is attributed to specific interactions between curcumin and OTA, primarily involving energy and electron transfer mechanisms in optical detection. In electrochemical detection, curcumin molecules form complexes with OTA molecules, increasing the binding affinity between OTA and the electrode surface. As a result, the presence of OTA in the electrolyte solution causes a greater change in the impedance of the double layer, which can be more easily detected by electrochemical impedance spectroscopy (EIS). Given their exceptional analytical performance and simple manufacturing process, our sensors hold great promise for OTA detection in beverages.

CRediT authorship contribution statement

Danilo M. dos Santos: Conceptualization, Data curation, Formal analysis, Investigation, Methodology, Validation, Writing – original draft, Writing – review & editing. **Fernanda L. Migliorini:** Conceptualization, Data curation, Formal analysis, Investigation, Methodology, Validation, Visualization, Writing – original draft, Writing – review & editing. **Andrey Coatrini-Soares:** Investigation, Methodology, Writing – original draft, Writing – review & editing. **Juliana C. Soares:** Investigation, Methodology, Writing – review & editing. **Luiz H.C. Mattoso:** Funding acquisition, Resources, Writing – review & editing. **Osvaldo N. Oliveira:** Funding acquisition, Resources, Writing – review & editing. **Daniel S. Correa:** Conceptualization, Funding acquisition, Project administration, Resources, Supervision, Writing – original draft, Writing – review & editing.

Declaration of competing interest

The authors declare that they have no known competing financial interests or personal relationships that could have appeared to influence the work reported in this paper.

Data availability

Data will be made available on request.

Acknowledgments

The authors acknowledge the financial support from Fundação de Amparo à Pesquisa do Estado de São Paulo (FAPESP) (2017/20973-4, 2017/21791-7, 2018/18953-8, 2018/22214-6, 2020/14946-7), Conselho Nacional de Desenvolvimento Científico e Tecnológico (CNPq) (151567/2022-0, 102124/2022-1), MCTI-SisNano (CNPq/402287/2013-4), CAPES, INEO and Rede Agronano-EMBRAPA from Brazil.

Supplementary materials

Supplementary material associated with this article can be found, in the online version, at doi:10.1016/j.snr.2023.100184.

References

[1] X. Yin, S. Wang, X. Liu, C. He, Y. Tang, Q. Li, J. Liu, H. Su, T. Tan, Y. Dong, Aptamer-based colorimetric biosensing of ochratoxin A in fortified white grape wine sample using unmodified gold nanoparticles, Anal. Sci. 33 (2017) 659–664, https://doi.org/10.2116/analsci.33.659.

[2] S. Agriopoulou, E. Stamatelopoulou, T. Varzakas, Advances in occurrence, importance, and mycotoxin control strategies: prevention and detoxification in foods, Foods 9 (2020), https://doi.org/10.3390/foods9020137.

[3] R.A. El-Sayed, A.B. Jebur, W. Kang, M.A. El-Esawi, F.M. El-Demerdash, An overview on the major mycotoxins in food products: characteristics, toxicity, and analysis, J. Future Foods 2 (2022) 91–102, https://doi.org/10.1016/j.jfutfo.2022.03.002.

[4] Y. Alhamoud, D. Yang, S.S. Fiati Kenston, G. Liu, L. Liu, H. Zhou, F. Ahmed, J. Zhao, Advances in biosensors for the detection of ochratoxin A: bio-receptors, nanomaterials, and their applications, Biosens. Bioelectron. 141 (2019) 111418, https://doi.org/10.1016/j.bios.2019.111418.

[5] C. Jiang, L. Lan, Y. Yao, F. Zhao, J. Ping, Recent progress in application of nanomaterial-enabled biosensors for ochratoxin A detection, TrAC - Trends Anal. Chem. 102 (2018) 236–249, https://doi.org/10.1016/j.trac.2018.02.007.

[6] P. Kumar, D.K. Mahato, B. Sharma, R. Borah, S. Haque, M.M.C. Mahmud, A. K. Shah, D. Rawal, H. Bora, S. Bui, Ochratoxins in food and feed: occurrence and its impact on human health and management strategies, Toxicon 187 (2020) 151–162, https://doi.org/10.1016/j.toxicon.2020.08.031.

[7] S.N. Chulze, C.E. Magnoli, A.M. Dalcero, Occurrence of ochratoxin A in wine and ochratoxigenic mycoflora in grapes and dried vine fruits in South America, Int. J. Food Microbiol. 111 (2006), https://doi.org/10.1016/j.ijfoodmicro.2006.02.006.

[8] S.C. Duarte, A. Pena, C.M. Lino, A review on ochratoxin A occurrence and effects of processing of cereal and cereal derived food products, Food Microbiol. 27 (2010) 187–198, https://doi.org/10.1016/j.fm.2009.11.016.

[9] A.L. Gonzalez, V.A. Lozano, G.M. Escandar, M.A. Bravo, Determination of ochratoxin A in coffee and tea samples by coupling second-order multivariate calibration and fluorescence spectroscopy, Talanta 219 (2020) 121288, https://doi.org/10.1016/j.talanta.2020.121288.

[10] D. Flajs, A.M. Domijan, D. Ivić, B. Cvjetković, M. Peraica, ELISA and HPLC analysis of ochratoxin A in red wines of Croatia, Food Control 20 (2009) 590–592, https://doi.org/10.1016/j.foodcont.2008.08.021.

[11] L. Campone, A.L. Piccinelli, R. Celano, I. Pagano, M. Russo, L. Rastrelli, Rapid and automated on-line solid phase extraction HPLC–MS/MS with peak focusing for the determination of ochratoxin A in wine samples, Food Chem. 244 (2018) 128–135, https://doi.org/10.1016/j.foodchem.2017.10.023.

[12] A.L. Sun, Y.F. Zhang, G.P. Sun, X.N. Wang, D. Tang, Homogeneous electrochemical detection of ochratoxin A in foodstuff using aptamer–graphene oxide nanosheets and DNase I-based target recycling reaction, Biosens. Bioelectron. 89 (2017) 659–665, https://doi.org/10.1016/j.bios.2015.12.032.

[13] Y. Wei, J. Zhang, X. Wang, Y. Duan, Amplified fluorescent aptasensor through catalytic recycling for highly sensitive detection of ochratoxin A, Biosens. Bioelectron. 65 (2015) 16–22, https://doi.org/10.1016/j.bios.2014.09.100.

[14] P.K. Kalambate, Z. Rao, J.Wu Dhanjai, Y. Shen, R. Boddula, Y. Huang, Electrochemical (bio) sensors go green, Biosens. Bioelectron. 163 (2020) 112270, https://doi.org/10.1016/j.bios.2020.112270.

[15] H. Tai, Z. Duan, Y. Wang, S. Wang, Y. Jiang, Paper-Based Sensors for Gas, Humidity, and Strain Detections: a Review, ACS Appl. Mater. Interfaces 12 (2020) 31037–31053, https://doi.org/10.1021/acsami.0c06435.

[16] V. Krikstolaityte, R. Ding, E.Chua Hui Xia, G. Lisak, Paper as sampling substrates and all-integrating platforms in potentiometric ion determination, TrAC - Trends Anal. Chem. 133 (2020) 116070, https://doi.org/10.1016/j.trac.2020.116070.

[17] H. Chen, O. Hu, Y. Fan, L. Xu, L. Zhang, W. Lan, Y. Hu, X. Xie, L. Ma, Y. She, H. Fu, Fluorescence paper-based sensor for visual detection of carbamate pesticides in food based on CdTe quantum dot and nano ZnTPyP, Food Chem. 327 (2020), https://doi.org/10.1016/j.foodchem.2020.127075.

[18] S.K. Biswas, S. Chatterjee, S. Bandyopadhyay, S. Kar, N.K. Som, S. Saha, S. Chakraborty, Smartphone-Enabled Paper-Based Hemoglobin Sensor for Extreme Point-of-Care Diagnostics, ACS Sens. 6 (2021) 1077–1085, https://doi.org/10.1021/acssensors.0c02361.

[19] T. Naghdi, H. Golmohammadi, M. Vosough, M. Atashi, I. Saeedi, M.T. Maghsoudi, Lab-on-nanopaper: an optical sensing bioplatform based on curcumin embedded in bacterial nanocellulose as an albumin assay kit, Anal. Chim. Acta 1070 (2019) 104–111, https://doi.org/10.1016/j.aca.2019.04.037.

[20] N. Pourreza, H. Golmohammadi, Application of curcumin nanoparticles in a lab-on-paper device as a simple and green pH probe, Talanta 131 (2015) 136–141, https://doi.org/10.1016/j.talanta.2014.07.063.

[21] Q.H. Zhu, G.H. Zhang, W.L. Yuan, S.L. Wang, L. He, F. Yong, G.H. Tao, Handy fluorescent paper device based on a curcumin derivative for ultrafast detection of peroxide-based explosives, Chem. Commun. 55 (2019) 13661–13664, https://doi.org/10.1039/c9cc06737j.

[22] K. Nagahama, T. Utsumi, T. Kumano, S. Maekawa, N. Oyama, J. Kawakami, Discovery of a new function of curcumin which enhances its anticancer therapeutic potency, Sci Rep 6 (2016) 1–14, https://doi.org/10.1038/srep30962.

[23] X. Cai, Z. Fang, J. Dou, A. Yu, G. Zhai, Bioavailability of quercetin: problems and promises, Curr. Med. Chem. 20 (2013) 2572–2582, https://doi.org/10.2174/09298673113209990120.

[24] Y.J. Wang, M.H. Pan, A.L. Cheng, L.I. Lin, Y.S. Ho, C.Y. Hsieh, J.K. Lin, Stability of curcumin in buffer solutions and characterization of its degradation products, J. Pharm. Biomed. Anal. 15 (1997) 1867–1876, https://doi.org/10.1016/S0731-7085(96)02024-9.

[25] M. Griesser, V. Pistis, T. Suzuki, N. Tejera, D.A. Pratt, C. Schneider, Autoxidative and cyclooxygenase-2 catalyzed transformation of the dietary chemopreventive agent curcumin, J. Biol. Chem. 286 (2011) 1114–1124, https://doi.org/10.1074/jbc.M110.178806.

[26] F.L. Migliorini, D.M. dos Santos, A.C. Soares, L.H.C. Mattoso, O.N. Oliveira, D. S. Correa, Design of a low-cost and disposable paper-based immunosensor for the rapid and sensitive detection of aflatoxin B1, Chemosensors 8 (2020) 87, https://doi.org/10.3390/CHEMOSENSORS8030087.

[27] R. Minghim, F.V. Paulovich, A. de Andrade Lopes, Content-based text mapping using multi-dimensional projections for exploration of document collections, Vis. Data Anal. 6060 (2006) 60600S, https://doi.org/10.1117/12.650880, 2006.

[28] F.V. Paulovich, M.L. Moraes, R.M. Maki, M. Ferreira, O.N. Oliveira, M.C.F. De Oliveira, Information visualization techniques for sensing and biosensing, Analyst 136 (2011) 1344–1350, https://doi.org/10.1039/c0an00822b.

[29] A.C. Soares, J.C. Soares, V.C. Rodrigues, O.N. Oliveira, L.H. Capparelli Mattoso, Controlled molecular architectures in microfluidic immunosensors for detecting: staphylococcus aureus, Analyst 145 (2020) 6014–6023, https://doi.org/10.1039/d0an00714e.

[30] X. Du, G. Wen, Z. Li, H.W. Li, Paper sensor of curcumin by fluorescence resonance energy transfer on nitrogen-doped carbon quantum dot, Spectrochim. Acta A Mol. Biomol. Spectrosc. 227 (2020), https://doi.org/10.1016/j.saa.2019.117538.

[31] M.C. Dos Santos, W.R. Algar, I.L. Medintz, N. Hildebrandt, Quantum dots for Förster Resonance Energy Transfer (FRET), TrAC - Trends Anal. Chem. 125 (2020), https://doi.org/10.1016/j.trac.2020.115819.

[32] Z. Hu, W.P. Lustig, J. Zhang, C. Zheng, H. Wang, S.J. Teat, Q. Gong, N.D. Rudd, J. Li, Effective detection of mycotoxins by a highly luminescent metal-organic framework, J. Am. Chem. Soc. 137 (2015) 16209–16215, https://doi.org/10.1021/jacs.5b10308.

[33] Comité de Direcção ICH, Validation of Analytical Procedures : text and Methodology Q2(R1), in: International Conference on Harmonization. 1994, 2005, p. 17. http://www.ich.org/fileadmin/Public_Web_Site/ICH_Products/Guidelines/Quality/Q2_R1/Step4/Q2_R1__Guideline.pdf.

[34] L.A. Currie, International Union of pure and applied chemistry nomenclature in evaluation of analytical methods including detection and quantification capabilities, cramers (Netherlands) national representatives: K. Doerffel (GDR), I. Giolito (Brazil), E. Grushka (Israel), W. E. Harris (Canada J. Stay. 67 (1995) 1699–1723. https://old.iupac.org/publications/pac/1995/pdf/6710x1699.pdf.

[35] L.R. Norton, Food and drug administration, Br. Med. J. 334 (2007) 55–56, https://doi.org/10.1136/bmj.39049.545880.BE.

[36] S. Chaiyo, E. Mehmeti, K. Žagar, W. Siangproh, O. Chailapakul, K. Kalcher, Electrochemical sensors for the simultaneous determination of zinc, cadmium and lead using a Nafion/ionic liquid/graphene composite modified screen-printed carbon electrode, Anal. Chim. Acta 918 (2016) 26–34, https://doi.org/10.1016/j.aca.2016.03.026.

[37] Y. Fu, L. Huang, S. Zhao, X. Xing, M. Lan, X. Song, A carbon dot-based fluorometric probe for oxytetracycline detection utilizing a Förster resonance energy transfer mechanism, Spectrochim. Acta A Mol. Biomol. Spectrosc. 246 (2021), https://doi.org/10.1016/j.saa.2020.118947.

[38] Z. Wu, B. Wang, Z. Cheng, X. Yang, S. Dong, E. Wang, A facile approach to immobilize protein for biosensor: self-assembled supported bilayer lipid

membranes on glassy carbon electrode, Biosens. Bioelectron. 16 (2001) 47–52, https://doi.org/10.1016/S0956-5663(00)00132-9.
[39] A. Inselberg, B. Dimsdale, Parallel coordinates: a tool for visualizing multi-dimensional geometry, (1990) 361–378. https://doi.org/10.1007/978-4-431-68057-4_3.
[40] J.C. Soares, F.M. Shimizu, A.C. Soares, L. Caseli, J. Ferreira, O.N. Oliveira, Supramolecular Control in Nanostructured Film Architectures for Detecting Breast Cancer, ACS Appl. Mater. Interfaces 7 (2015) 11833–11841, https://doi.org/10.1021/acsami.5b03761.
[41] R.G. Greenler, Infraredc study of adsorbed molecules on metal surfaces by reflection tehniques, J. Chem. Phys. 44 (1966) 310–315, https://doi.org/10.1063/1.1726462.
[42] W.G. Golden, D.S. Dunn, J. Overend, A method for measuring infrared reflection-Absorption spectra of molecules adsorbed on low-area surfaces at monolayer and submonolayer concentrations, J. Catal. 71 (1981) 395–404, https://doi.org/10.1016/0021-9517(81)90243-8.
[43] X. Chen, L.Q. Zou, J. Niu, W. Liu, S.F. Peng, C.M. Liu, The stability, sustained release and cellular antioxidant activity of curcumin nanoliposomes, Molecules 20 (2015) 14293–14311, https://doi.org/10.3390/molecules200814293.
[44] M. Tan, Introduction to infrared and raman spectroscopy, 3 rd, 1991. https://doi.org/10.1007/bf01731922.
[45] L. Liu, Q. Huang, Z.I. Tanveer, K. Jiang, J. Zhang, H. Pan, L. Luan, X. Liu, Z. Han, Y. Wu, "Turn off-on" fluorescent sensor based on quantum dots and self-assembled porphyrin for rapid detection of ochratoxin A, Sens. Actuators B Chem. 302 (2020), https://doi.org/10.1016/j.snb.2019.127212.
[46] Z. Lu, X. Chen, W. Hu, A fluorescence aptasensor based on semiconductor quantum dots and MoS2 nanosheets for ochratoxin A detection, Sens. Actuators B Chem. 246 (2017) 61–67, https://doi.org/10.1016/j.snb.2017.02.062.
[47] L. Lv, D. Li, R. Liu, C. Cui, Z. Guo, Label-free aptasensor for ochratoxin A detection using SYBR Gold as a probe, Sens. Actuators B Chem 246 (2017) 647–652, https://doi.org/10.1016/j.snb.2017.02.143.
[48] F. Malvano, D. Albanese, A. Crescitelli, R. Pilloton, E. Esposito, Impedimetric label-free immunosensor on disposable modified screen-printed electrodes for ochratoxin a, Biosens. (Basel) 6 (2016), https://doi.org/10.3390/bios6030033.
[49] F. Malvano, D. Albanese, R. Pilloton, M. Di Matteo, A highly sensitive impedimetric label free immunosensor for Ochratoxin measurement in cocoa beans, Food Chem. 212 (2016) 688–694, https://doi.org/10.1016/j.foodchem.2016.06.034.
[50] Y. Wang, G. Ning, Y. Wu, S. Wu, B. Zeng, G. Liu, X. He, K. Wang, Facile combination of beta-cyclodextrin host-guest recognition with exonuclease-assistant signal amplification for sensitive electrochemical assay of ochratoxin A, Biosens. Bioelectron. 124–125 (2019) 82–88, https://doi.org/10.1016/j.bios.2018.10.007.